PPIC PUBLIC POLICY INSTITUTE OF CALIFORNIA

SGMA-Ready Crops as a Low-Water Alternative to Fallowing

Technical Appendices

CONTENTS

Supported with funding from the S. D. Bechtel, Jr. Foundation and the Agriculture and Food Research Initiative, project award no. 2023-67019-39707, from the US Department of Agriculture's National Institute of Food and Agriculture. Any opinions, findings, conclusions, or recommendations expressed in this publication are those of the authors and should not be construed to represent any official USDA or US government determination or policy.

Appendix A. Evapotranspiration From Fallowed Fields and Winter Grains in the San Joaquin Valley

Introduction

Implementation of the Sustainable Groundwater Management Act in California's heavily agricultural San Joaquin Valley is expected to increase the extent of fallow or bare agricultural fields. The prospect of widespread fallowing has raised concerns about dust emissions, pests, and weeds, as well as lost economic opportunity of nearly $5 billion in agricultural GDP and 40–50,000 agricultural jobs (Escriva-Bou et al. 2023). In the report *SGMA-Ready Crops as a Low-Water Alternative to Fallowing* that accompanies this appendix, we examine the potential and scope for transitioning to winter grain cropping systems that, when managed with best practices for water-limited conditions, can keep agricultural lands in production with minimal water costs.

Transitioning agricultural lands to SGMA-ready cropping systems is an option for reducing the amount of land fallowed due to groundwater cutbacks. However, one hurdle to wider adoption has been the lack of clear understanding of 1) water use in water-limited cropping systems relative to both business-as-usual crop management and fallowed ground, and 2) water use in fallowed fields themselves.

When creating programs and rules to address groundwater demand, many local agencies assume that fallowing farmland is the only way to eliminate consumptive water use—often measured as evapotranspiration (ET). However, fallowed land is inefficient at capturing rainfall, and much of the rain received during the winter rainy season is subsequently lost from the soil as evaporation. Keeping crops in the ground and harvesting them early for forage products offers opportunities to make good use of water that would otherwise be lost to evaporation, while minimally impacting the overall water balance of a field.

Below we describe in more detail the results from two analyses of water use in fallowed fields relative to their winter-cropped counterparts. In the first analysis we examine a single field site in western Fresno County, where we directly measured evaporation from bare soil using two approaches: an eddy covariance flux tower and a weighing lysimeter at the site. We also compare these direct measurement methods with modeled estimates using publicly available meteorological data. In the second analysis, we use remote sensing tools and OpenET models estimates to compare ET from fallowed land and winter-cropped fields for larger regions (i.e., the San Joaquin River and Tulare Lake groundwater basins in the San Joaquin Valley). These results provide a benchmark for understanding water use from bare fallowed land and winter wheat produced with standard San Joaquin Valley management practices, illustrating the management windows that are most critical for reducing crop water use under water-limited conditions.

Direct measurement of evaporation on fallowed farmland

Field-specific consumptive water use measurements are required to refine water accounting frameworks and document progress towards SGMA sustainability goals. Although numerous studies have applied micrometeorological measurement techniques to measure consumptive water use for important crops, evapotranspiration (ET) from fallowed lands, including bare fields, has been less studied. To better characterize the uncertainty of measured and modeled soil evaporation (E) estimates for fallowed lands, we measured E over two consecutive winters using two different direct measurement techniques: an eddy covariance flux tower and an in-ground weighing lysimeter. The eddy covariance tower measures E by correlating vertical fluxes of air with concentrations of water vapor. The lysimeter measures evaporation by tracking the mass of a known volume of soil, assuming that lost mass is equivalent to the mass of water lost via evaporation.

The E measurements occurred across two consecutive winter seasons: November 2023 to April 2024 and November 2024 to April 2025. During each season, the instruments were set up in a bare fallow field at the University of California Westside Research and Extension Center (WSREC) in Five Points, CA. The E measurements from these instruments were complemented by precipitation gauges, soil moisture profiles, and a nearby weather station measuring solar radiation, temperature, and humidity. Precipitation was measured using 4 in-field rain gauges and a 5th CIMIS rain gauge in the adjacent field (DWR 2026). Soil moisture was measured using digital soil moisture sensors at depths of approximately 2 in, 20 in, and 40 in. These complementary measurements provided a benchmark for field-scale water balance estimates by informing measurement uncertainty and offering a point of comparison for modeled soil evaporation values. Post-processing techniques were applied to ensure quality control and make energy balance corrections.

We recorded 5.6 ± 0.17 inches of evaporation from October to April in the near-average rainfall year of 2023–24, which was 70.5 ± 10.6 percent of total rainfall, and 4.87 ± 0.16 inches of evaporation in the dry year of 2024–25 (100 percent of total rainfall). Results show good agreement between lysimeter and eddy covariance ET measurements for both seasons (Figures A1 and A2). Measurement methods were within 7 percent of each other for season 1, and within 22 percent of each other in season 2. The mean absolute difference between the two measurements was 26 percent for days with coincident high-quality measurements.

FIGURE A1

Direct measurements of soil evaporation in two years at the experimental site in western Fresno County

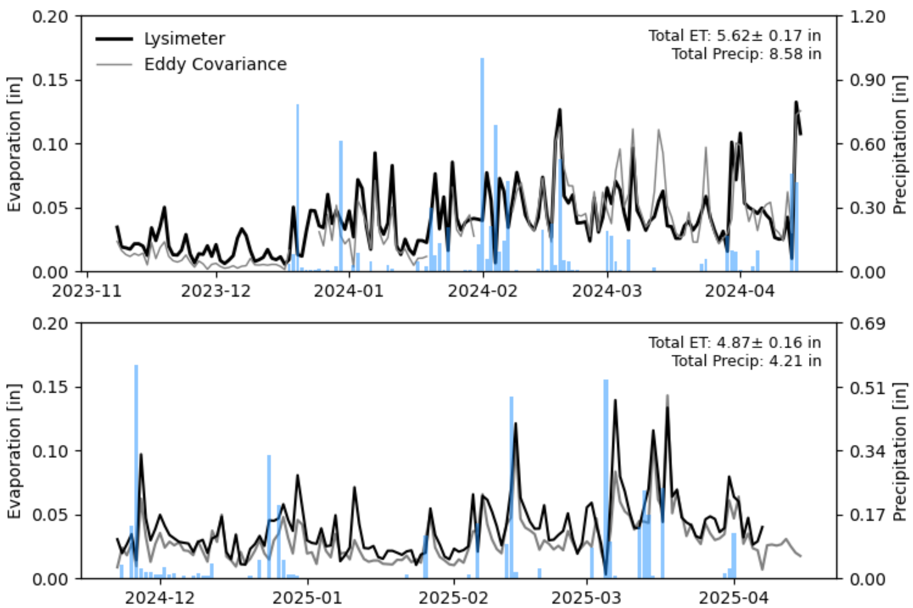

SOURCE: Author measurements.

NOTES: Shown are measurements of soil evaporation from an eddy covariance tower (gray line) and weighing lysimeter (black line), compared to precipitation (blue bars), from a fallow field at WSREC near Five Points, CA. Top row: data from the wet winter of 2023–24; bottom row: data from the "normal" winter of 2024–25.

FIGURE A2

Cumulative soil evaporation in two years at the experimental site in western Fresno County

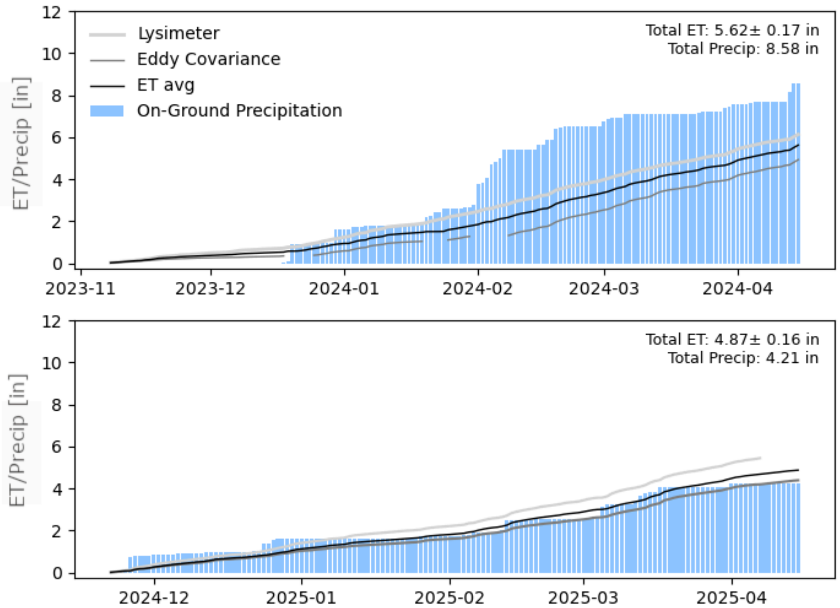

SOURCE: Author measurements.

NOTES: Shown are cumulative measurements of soil evaporation from an eddy covariance tower (dark gray line) and weighing lysimeter (light gray line), compared to cumulative precipitation (blue bars), from a fallow field at WSREC near Five Points, CA. The black line indicates the average ET between the two measurement methods. Top row: data from the wet winter of 2023–24; bottom row: data from the "normal" winter of 2024–25.

We also compared modeled E values to ground measurements to assess the uncertainty of current models. E was modeled using the FAO-56 dual-crop coefficient approach, where a water balance is used to determine the soil evaporation coefficient (or K_e; Allen et al., 1998). Inputs for the FAO-56 model included potential evapotranspiration (ET_o) and precipitation data sourced from either the nearby CIMIS station—referred to below as "in situ" measurements—or a gridded weather data product (gridMET; Abatzoglou et al., 2011).

Table A1 shows the accuracy of the model input relative to the measured soil evaporation values. The E values modeled using in situ data produced more accurate estimates compared to those modeled using the gridded product. Differences in model results were primarily driven by differences in precipitation. Overall, the models performed adequately in modeling E immediately after rainfall events, and in situ measurements improved their accuracy. However, eddy covariance and lysimeter measurements of E were higher than the FAO model estimates of E for the time between rainfall events.

TABLE A1

Mean difference between modeled and directly measured soil evaporation

Model	FAO-Ke (gridMET)		FAO-Ke (CIMIS)	
Measurement	Lysimeter	Eddy Cov.	Lysimeter	Eddy Cov.
Mean Difference (%)	-21.36	-14.67	-12.81	1.28

NOTES: Soil evaporation was modeled using the FAO-56 dual crop coefficient method informed either by gridded ET_o and precipitation (gridMET) or on ground measurements of ET_o and precipitation from a reference weather station (CIMIS). Modeled E was then compared to each direct measurement technique—lysimeter or eddy covariance—and the mean difference (%) reported. Statistics reflect combined 2023–24 and 2024–25 seasons.

Remotely sensed evapotranspiration of fallowed land and winter wheat at the basin scale

Alongside direct measurement techniques like those described above, remote sensing provides a valuable tool for estimating components of the terrestrial water balance and characterizing water dynamics at larger scales and at nearly continuous time intervals. OpenET produces publicly available gridded ET estimates at 30m spatial resolution at daily and monthly timescales (Melton et al., 2022; Volk et al., 2024). The ET data produced by OpenET reflect water inputs from precipitation, irrigation, or water stored in the soil. When ET exceeds precipitation, it indicates that rainfall alone is insufficient to meet crop water demand, requiring irrigation or depletion of stored soil moisture. With remote sensing approaches, we cannot know the exact management practices used at all locations. But we can use the difference between estimated ET and precipitation—or net water input—as a conservative indicator that supplementary irrigation was required to support crop development.

Here, we combine OpenET ensemble ET values with gridMET precipitation to examine how winter cropping decisions influence seasonal water balances in the San Joaquin Valley. We focus on winter wheat, the dominant winter crop in the region. Acreage of winter wheat and fallow land exhibits pronounced interannual variability that closely tracks water availability. As shown in Figure A3, fallowed acreage increased during dry years, such as the 2021–22 drought period, whereas winter wheat acreage generally expanded in wetter years such as 2023 when greater precipitation was available to support winter crop establishment and growth.

FIGURE A3

Fallow and winter wheat acreage mirrors precipitation trends

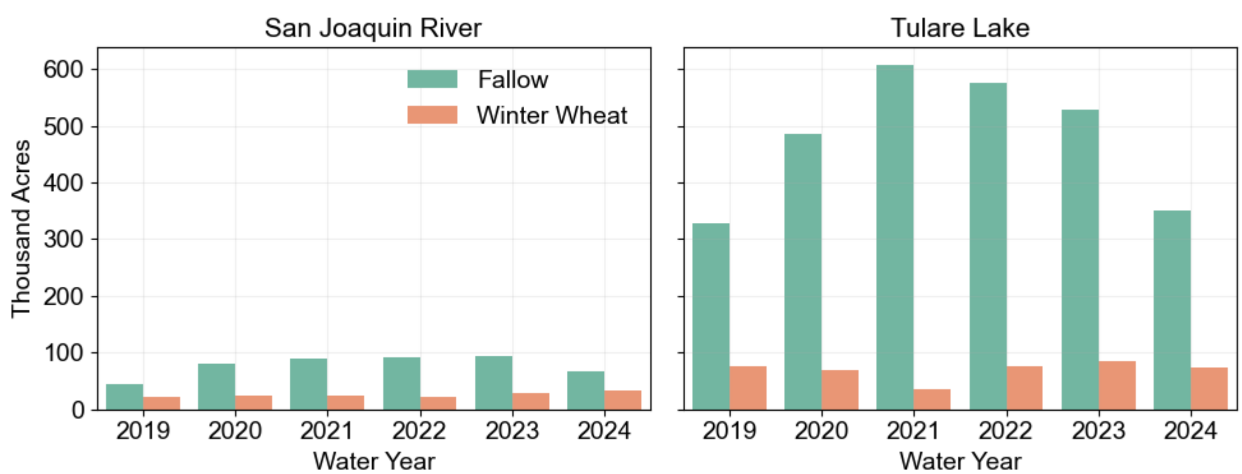

SOURCE: 2024 Statewide Crop Mapping (DWR 2024).

NOTES: Shown are acreage estimates for fallowed land and winter wheat crops in the San Joaquin River and Tulare Lake basins in the San Joaquin Valley. Fallowed acreage tends to increase during drought years, e.g., water years 2020–22, while winter crop acreage increases in years with plentiful rainfall (e.g., water year 2023 in Tulare Lake basin and 2024 in San Joaquin River basin).

We sourced OpenET (v2.0) data for every fallow and winter wheat field in the San Joaquin River and Tulare Lake groundwater basins. This analysis focused on water years 2021 (dry), 2023 (wet), and 2024 (average), representing contrasting hydrologic conditions in the San Joaquin Valley. The resulting dataset included parcel-level actual evapotranspiration (ET) from the OpenET ensemble, Landsat-derived normalized difference vegetation index (NDVI, a measure of plant greenness that can be used to classify remotely sensed land cover types; USGS 2026), and precipitation from gridMET, at a monthly time step.

We used several quality control procedures to ensure ET data reliability, minimize the influence of misclassified fields, and ensure that observed differences reflected management rather than data or classification biases. First, to maximize ET reliability, small fields (<5 acres) were excluded due to potential edge-effect bias associated with the resolution of satellite inputs. Second, fields with consistently low or invalid vegetation signals were removed by retaining only fields with positive (>0) NDVI values. To address specific misclassification scenarios, targeted filters were then applied to exclude the following fields: (1) fields classified as fallow that exhibited unusually high NDVI values (≥0.55), which would indicate fields that were not bare or minimally vegetated fields; (2) winter wheat fields with NDVI >0.6 after May, which would indicate double-cropped fields (e.g., wheat followed by corn); and (3) winter wheat fields with low peak NDVI (<0.5) during the primary growing period (March–April), which would indicate poorly established or misclassified fields. Collectively, these quality control steps produced a more consistent sample of winter wheat and fallow fields. After the filters were applied, we retained 900 fallow fields and 500 winter wheat fields in the San Joaquin River basin, and 4,900 fallow fields and 700 winter wheat fields in the Tulare Lake basin.

To evaluate the impact of management practices—primarily irrigation—on winter wheat water balance, we used monthly mean NDVI as an indicator of crop canopy development. For each water year and basin, we calculated field-level maximum seasonal NDVI and classified fields based on quartiles of the distribution. Fields in the upper quartile (≥75th percentile) were categorized as well-watered (including healthy wheat fields in locations where rainfall alone or rainfall + irrigation would have been sufficient to fully meet crop water requirements), whereas fields in the lower quartile (≤25th percentile) were classified as stressed. We regarded the stressed classification as the closest equivalent to the water-limited winter cereal management systems we describe in the accompanying report—systems that are not currently widely practiced in these regions.

As shown in Figure A4, NDVI increases through the winter and spring, reaches a peak during March–April (common early forage harvest time), and then declines rapidly in May and June (common late forage or grain harvest time). Well-watered fields exhibit substantially higher peak NDVI (> 0.75) and greater canopy persistence relative to stressed fields. The NDVI trajectories show how most winter wheat fields reach maturity and start to dry down in May, as reflected by the sharp decline in NDVI (lower "greenness" values from the drying crop). In contrast, fallow fields maintain consistently low NDVI throughout the water year, supporting their classification as bare, uncropped fields.

FIGURE A4

Monthly "greenness" indices classify fields as well-watered winter wheat, stressed wheat, or fallow

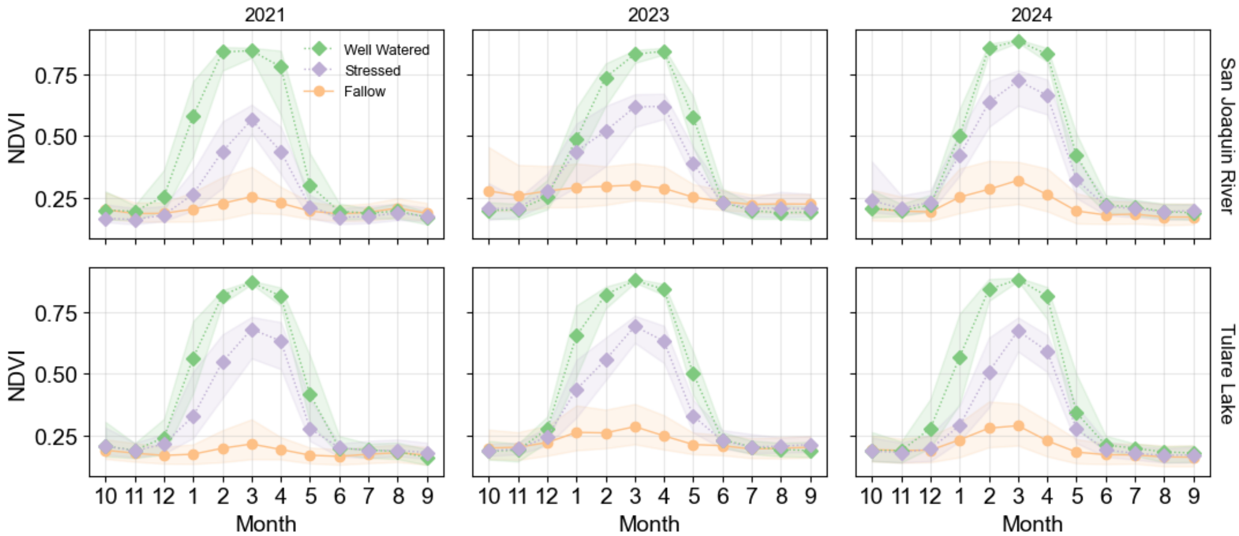

SOURCES: Landsat (NDVI); DWR (2024 land use).

NOTES: Normalized Difference Vegetation Index (NDVI) quantifies vegetation greenness derived from satellite imagery and is expressed as an index ranging from 0–1. Points represent monthly maximum NDVI for selected fields classified as fallow and well-watered or stressed winter wheat for 2021, 2023, and 2024 across the San Joaquin River (top), and Tulare Lake (bottom) basins. Shaded regions represent the interquartile range of median monthly mean NDVI. The three years represent varying hydrologic conditions in these regions: dry (2021), near-average (2024), and wet (2023). Timeseries are arranged by water years, which begin in October of the calendar year.

Comparing cumulative ET among land categories across years and subbasins reveals strong sensitivity to hydrologic conditions (Figure A5). In 2021, a critically dry year characterized by low precipitation and high evaporative demand, cumulative ET in the San Joaquin River basin remained comparatively low, particularly for stressed winter wheat fields. These observations are consistent with reduced crop canopy development under water-limited conditions. In contrast, although the Tulare Lake basin experienced similar drought conditions, cumulative ET for winter wheat fields was higher than in the San Joaquin River region, indicating regional differences in crop water use, and, likely, management practices and availability of water for supplemental irrigation under drought.

In 2023, a wet year, cumulative ET trajectories for well-watered, stressed, and fallow fields were comparable early in the season and remained closer throughout the water year relative to the other two years. This convergence reflects reduced water limitation during early growth stages. However, divergence among winter wheat categories becomes evident during March–April, coinciding with peak canopy development and increased transpiration, when healthy crops exhibit accelerated ET accumulation relative to stressed and fallow fields. In 2024, a near-average water year, cumulative ET patterns fall between the dry and wet extremes, with only moderate separation among management categories.

Across basins and years, total ET for fully irrigated winter wheat by the end of the typical grain harvest period (June) ranged from approximately 19 to 25 inches, whereas stressed wheat ET ranged from roughly 12 to 19 inches depending on water year type and region. The largest differences in cumulative ET consistently emerged during March–April, highlighting the importance of the timing of peak canopy development in determining seasonal consumptive water use.

FIGURE A5

Cumulative ET depends on region and hydrologic conditions

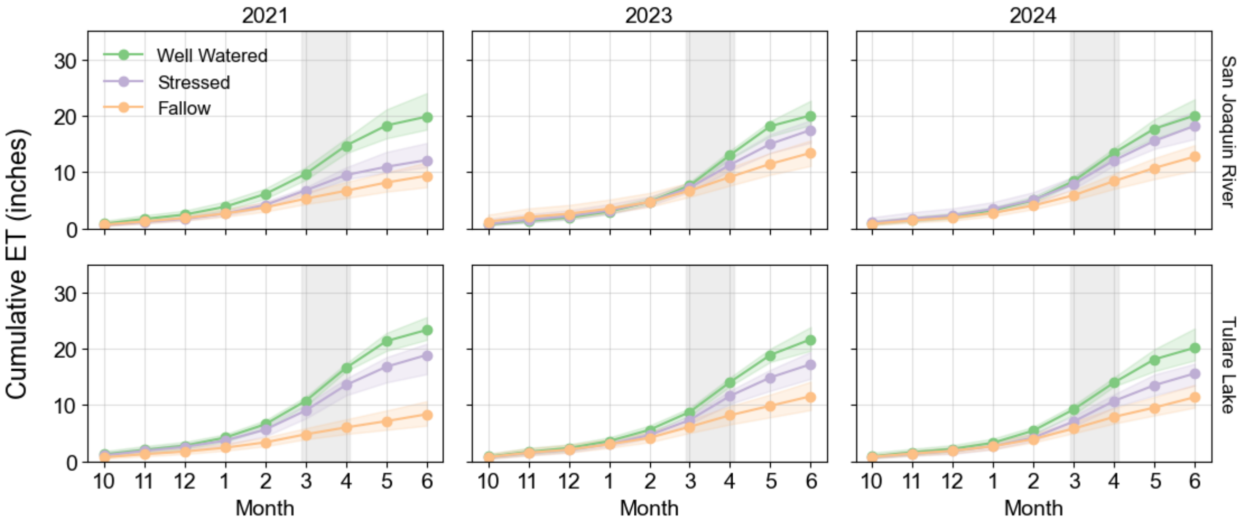

SOURCES: Landsat (NDVI); DWR (2024 land use); OpenET (cumulative ET).

NOTES: Monthly cumulative evapotranspiration (ET) for fully irrigated and stressed winter wheat and fallow fields in the San Joaquin River and Tulare Lake groundwater basins during water years 2021 (dry), 2023 (wet), and 2024 (near-average rainfall). Colored shaded regions represent interquartile ranges. The gray, vertical shaded region indicates the March–April window when ET accumulates the fastest. This timeframe also coincides with typical winter wheat forage harvest windows, whereas most winter wheat grain is harvested in June.

To further evaluate water balance implications and basin-scale management tradeoffs, we examined net water input across land management categories and regions (Figure A6). Net water input is the difference between cumulative precipitation (i.e., water inputs) and ET (i.e., water losses). Positive values indicate periods when cumulative rainfall exceeds water loss to the atmosphere via ET, suggesting that excess water may be stored in the soil or drain deeply to recharge aquifers. Negative values indicate that crop ET exceeded cumulative precipitation; we assume that the balance of the crop water requirement not met by precipitation would have been met by supplementary irrigation or depletion of stored soil water.

In the critically dry year of 2021, net water input becomes strongly negative by March–April for well-watered winter wheat in both basins, with deficits reaching approximately 15 inches in the San Joaquin River basin and nearly 20 inches in Tulare Lake. Stressed fields exhibit smaller but still substantial deficits (approximately 7 to 15 inches), while fallow fields show comparatively minor declines. In the wet year (2023), net water input remains positive or near zero through much of the winter across all categories, indicating that precipitation largely met crop water demand and likely supported groundwater recharge. Divergence among management classes emerges during March–April, when peak vegetative development increases transpiration and drives net water input downward, particularly for well-watered winter wheat fields. In contrast, stressed fields remain closer to a neutral net input consistent with production supported predominantly by precipitation.

In the near-average year (2024), a similar pattern was observed in both basins, with net water input declining during April for both well-watered and water-limited winter wheat fields. By June, deficits reached approximately 8 to 12 inches for well-watered fields, indicating moderate need for supplementary irrigation relative to the critically dry year. Negative net water input values during peak growth (March–April) underscore the importance of late-winter and early-spring management decisions in shaping seasonal water deficits.

FIGURE A6

Peak crop growth windows dictate the balance between positive and negative net water input

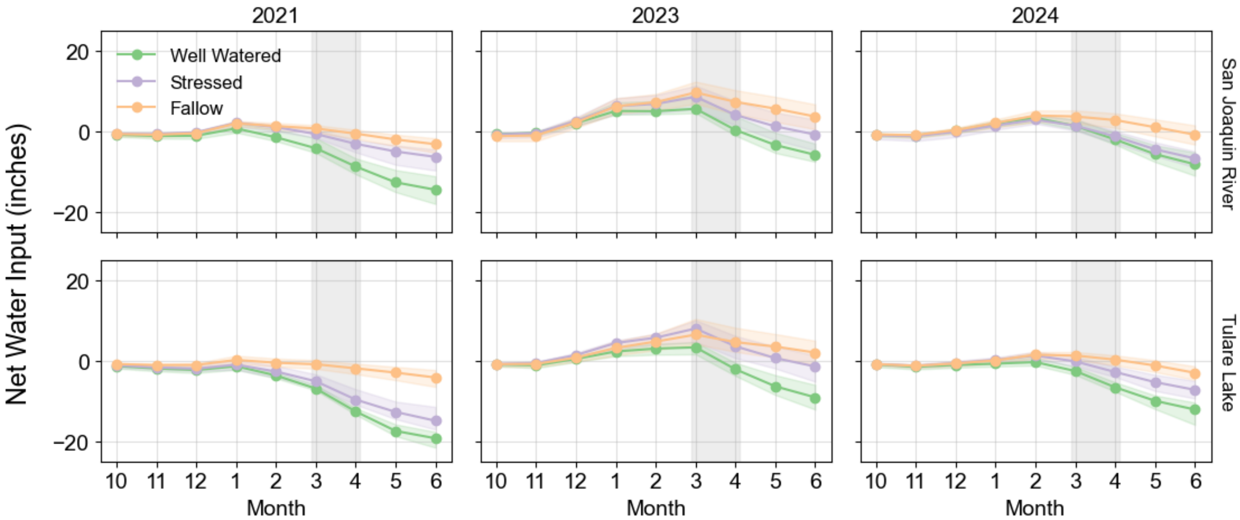

SOURCES: Landsat (NDVI); DWR (2024 land use); OpenET (cumulative ET).

NOTES: Net water input is calculated as monthly cumulative precipitation minus ET for well-watered and stressed winter wheat and fallow fields in the San Joaquin River and Tulare Lake basins during water years 2021 (dry), 2023 (wet), and 2024 (near-average). Colored shaded regions represent interquartile ranges. The gray, vertical shaded region indicates the March–April window when ET accumulates the fastest and net ET can quickly shift from positive to negative. This timeframe also coincides with typical winter wheat forage harvest windows, whereas most winter wheat grain is harvested in June.

Insights from ET measurements for SGMA-ready cropping system transitions

Across years, the most pronounced declines in the climatic water balance consistently occured during March–April, coinciding with peak vegetative growth and maximum transpiration demand (summarized in Figure A7). This window represents the period when seasonal water deficits begin to develop and when differences in management practices or water availability for supplemental irrigation manifest as differences in crop canopy development and therefore ET accumulation and consumptive use. Notably, in both the wet (2023) and average (2024) years, net water input remains near neutral until approximately March, indicating that precipitation largely meets crop water demand prior to peak vegetative development. Additionally, in the wet year (2023), both well-watered and water-limited winter wheat fields exhibited net water use trajectories similar to fallow fields.

These results have important implications for adapting management systems to water-limited conditions under SGMA, suggesting that harvest timing is an important management lever. For example, earlier harvest of winter cereal crops as forage products during this March–April window (instead of harvest for grain in June) could largely avoid seasonal water deficits while resulting in productive outputs and economic returns. However, in drier years and in drier regions (such as the Tulare Lake basin shown here), larger negative differences between ET demand and precipitation may emerge earlier, especially for well-watered crops. In these cases it will be important to adapt management practices to water-limited conditions, e.g., by planting winter cereals early, applying small amounts of supplemental irrigation (~4 inches), and harvesting early for forage products instead of grain (see report).

FIGURE A7

Net water use is often positive in the March–April window, when winter wheat can be harvested for forage

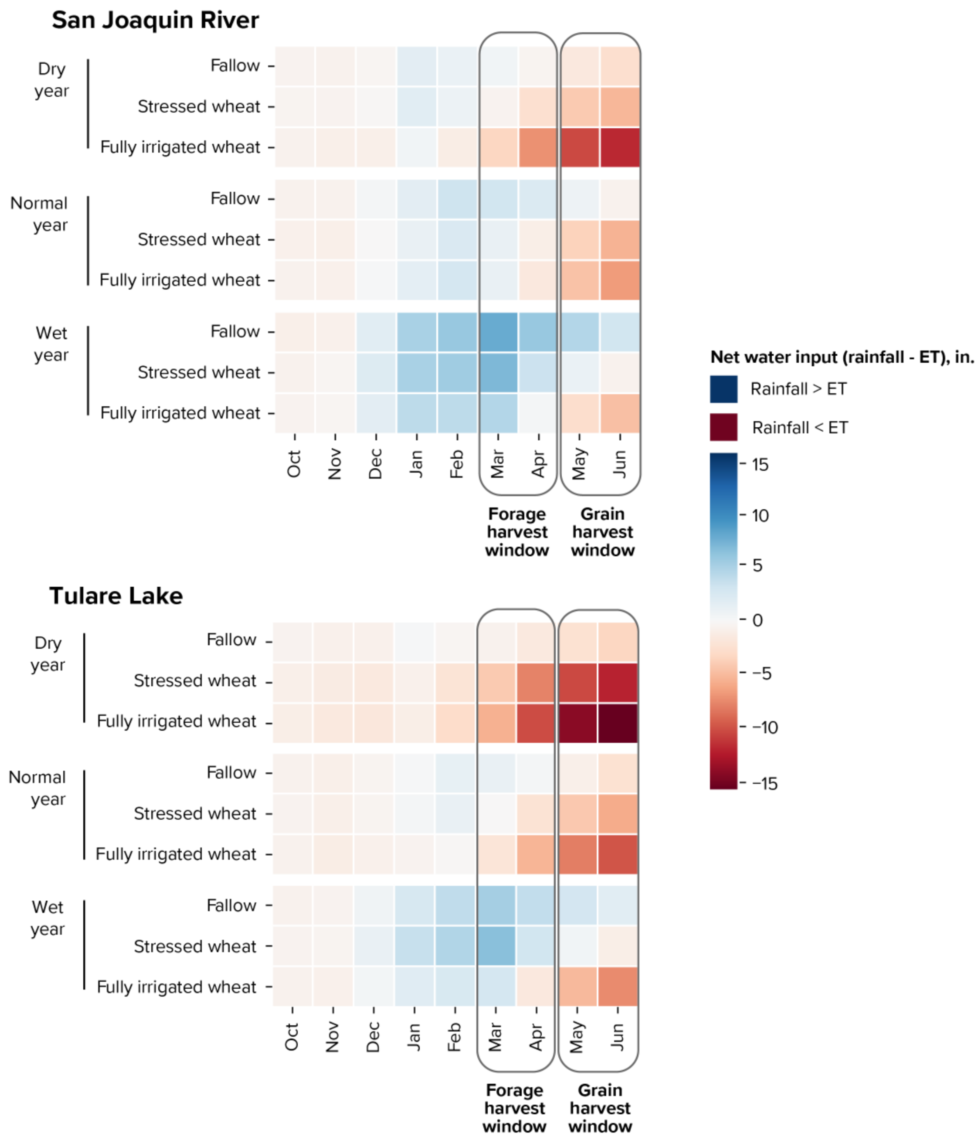

SOURCES: Landsat (NDVI); DWR (2024 land use); OpenET (cumulative ET)

NOTES: Net water input is calculated as median cumulative precipitation minus ET (inches) by land management class (well-watered, stressed, or fallow) and basin (San Joaquin River and Tulare Lake) for water years 2021 (dry), 2023 (wet), and 2024 (near-average). Positive net water input values indicate that precipitation exceeds water use via ET. Negative values indicate net water loss, or ET values exceeding water input from precipitation. Outlined columns denote 1) the March–April period when peak vegetative growth (and thus ET) coincides with the wheat forage harvest window, and 2) the May–June period corresponding to the wheat grain harvest window, when cumulative ET often exceeds precipitation suggesting that the crop was irrigated to meet water demands.

Appendix B. Water Productivity and Management of Winter Forages in the San Joaquin Valley

Introduction

California's agricultural sector is facing major transitions related to implementing the Sustainable Groundwater Management Act (SGMA). The San Joaquin Valley is the state's leading agricultural region—and also the region with the most critically overdrafted groundwater basins. Bringing basins into balance will require a combination of new supplies and reduced demand, including the removal of up to 900,000 acres of cropland from irrigated production.

Finding alternative uses for this land will help to soften SGMA's impact on the regional agricultural economy and quality of life for rural communities that depend on agriculture. As described in previous PPIC and University of California research, keeping agricultural land in production with non-irrigated or minimally irrigated cropping systems is one such alternative that would offer opportunities to earn income on otherwise idle land, while mitigating nuisances—such as dust, pests, and weeds—from widespread fallowing (Peterson, Pittelkow, and Lundy 2022).

As water-limited cropping systems are not commonly practiced in the San Joaquin Valley today, there is a need to understand management approaches and practical agronomic considerations that support their viability in the valley's unique growing conditions. This includes testing key management levers such as planting date, harvest stage, and irrigation, which we do in the experimental crop trials discussed in this appendix.

This document is a supplement to the PPIC report *SGMA-Ready Crops as a Low-Water Alternative to Fallowing*. It details experimental methods and analytical details underlying the results presented in the section titled "When Irrigation is Limited, Crop Management Matters," which discusses water productivity of forage products and depletion of soil moisture in winter cropped and fallow fields.

Testing small grain crop management strategies under water-limited conditions

In previous work, we tested management scenarios for water-limited conditions using crop models calibrated with empirical data from winter wheat field trials at representative sites in the San Joaquin Valley (Peterson, Pittelkow, and Lundy 2022 and 2023). Model outputs provided conservative estimates of wheat biomass and grain yields with no or minimal irrigation: 0, 4, or 8 inches applied via flood system. This exercise indicated key management factors that could improve crop performance—and particularly water productivity—under very limiting water conditions: early planting, targeting forage over grain harvest, and early-season supplemental irrigation to support crop establishment.

The research described in this appendix and the accompanying report builds upon these earlier results, implementing the management practices under field conditions. We present selected results below, providing further evidence to support our findings on best management approaches for water-limited growing conditions in the San Joaquin Valley.

Experimental design

We conducted two years of field trials at the University of California West Side Research and Extension Center (WSREC) near Five Points, California. Average precipitation in Five Points is 7.6 inches per year (PRISM

Climate Group). The soil is a Panoche clay loam (SSURGO, 2026). Over two winter growing seasons (2023–24 and 2024–25), we tested eight combinations of planting date and irrigation treatment, creating eight unique water environments, outlined in Table B1.

TABLE B1
Planting date and irrigation combinations tested for water-limited winter small grain crops at WSREC

Season	Treatment description	Planting date	Forage harvest date	Irrigation applied (in.)	Precipitation (in.)
2023–2024	Early planting w/ establishment irrigation	10/18/2023	03/08/2024	3.5	6.3
2023–2024	Mid planting w/ establishment irrigation	11/14/2023	04/03/2024	3.5	7.1
2023–2024	Late planting w/ establishment irrigation	12/12/2023	04/19/2024	3.5	8.6
2023–2024	Mid planting, rainfed	12/18/2023	05/01/2024	0	8.6
2023–2024	Late planting, rainfed	01/18/2024	05/01/2024	0	8.6
2024–2025	Early planting w/ establishment irrigation	10/21/2024	03/19/2025	3.5	3.9
2024–2025	Mid planting, rainfed	11/26/2024	04/09/2025	0	3.9
2024–2025	Late planting w/ establishment irrigation	12/22/2024	04/16/2025	3.5	3.9

NOTES: We tested eight unique planting environments across the 2023–24 and 2024–25 winter growing season in Five Points, California. Planting date represents the date of seed germination, which is either the date of irrigation for irrigated fields or the date of the first germinating rainfall for rainfed fields. Irrigation was applied at crop establishment, 1–4 days after sowing. Precipitation is the sum of rainfall received from germination date to forage harvest date.

Irrigation treatments included either minimal irrigation (referred to as the "establishment irrigation" treatment in this appendix) or no irrigation (referred to as the "rainfed" treatment). For the establishment irrigation treatment, 3.5 inches of irrigation were applied via flood irrigation immediately after planting. Planting dates were chosen to represent a standard planting schedule for this region (typically mid- to late November), as well as an earlier (October) and later (December–January) planting date. We considered the exact planting date to be the date of seed germination, as seeds will remain dormant in dry soil until they receive an activating amount of rainfall or irrigation. Germination date was determined either by the date of establishment irrigation (irrigated treatments), or the first germinating rainfall (rainfed treatments).

Within each environment, we grew four varieties in each of three winter small grain crop types, for a total of twelve varieties. Winter small grain crops included wheat (*Triticum aestivum*), barley (*Hordeum vulgare*), and triticale (× *Triticosecale*). Selected varieties within each crop type represented a range of developmental rates. Potential outputs from these crop varieties include green chop, silage, hay products intended for forage, and grain products intended for milling, malting, or livestock feed. Varieties were planted in randomized plots of approximately 20 square feet in area and seeded at a rate of 1.5 million seeds per acre.

The experimental field used in the first year was previously planted in sugar beets. Residue from the sugar beet harvest was disked in before field preparation for this experiment. In the second year, the experimental field preparation followed three years of fallow. Pre-season field preparation included tillage and fertilizer application. In both years, 100 pounds per acre of monoammonium phosphate fertilizer was applied prior to the first planting date and harrowed into the soil. In the 2023–24 season, 109 pounds per acre of urea fertilizer were applied in late January ahead of rain events.

Weather conditions

The two trial years included notably different rainfall amounts. In the first season (October 2023 through June 2024), precipitation was 116 percent of the historical average and well-distributed across the entire growing season; in the second (October 2024 through June 2025), precipitation was 46 percent of the average (Figure B1).

FIGURE B1

Seasonal precipitation at Five Points, CA near WSREC in 2023–24 and 2024–25 relative to the historical average

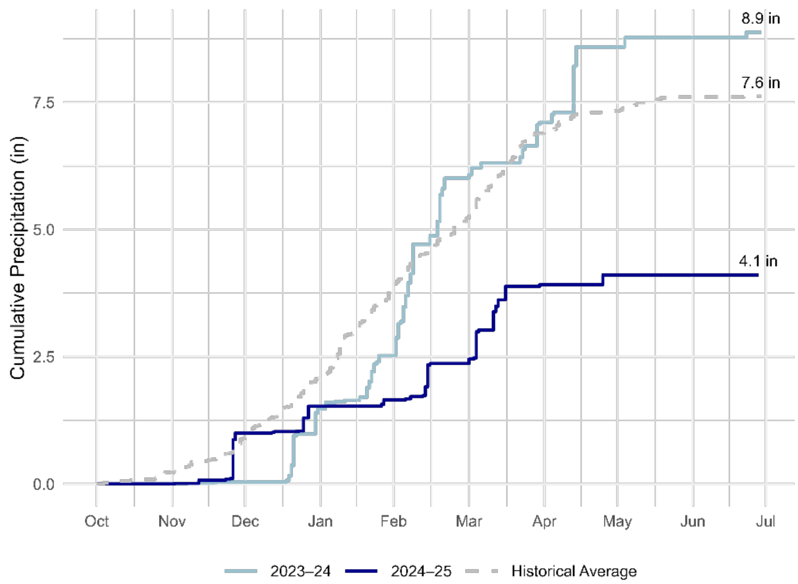

SOURCE: PRISM (daily rainfall).

NOTES: Precipitation is shown for the 2023–24 and 2024–25 winter growing seasons in Five Points, California, near the WSREC field trials. The winter growing season spans October 1–June 30. The solid light blue line is cumulative precipitation for the 2023–24 season. The solid dark blue line is cumulative precipitation for the 2024–25 season. The dotted grey line is the cumulative average precipitation for the past 10 years.

Estimating forage yields

Crops were harvested when the average growth stage among varieties was close to soft dough growth stage—a late-stage forage that occurs after grain heads have emerged but before grain ripening is complete. We harvested subplots of the forage by hand or mechanical harvester and weighed samples in the field. We then oven-dried the samples at 120ºF until they reached a stable weight, then weighed again to determine moisture content. We calculated final forage yields as pounds of dry forage biomass per acre at 10 percent moisture content (similar to the 12–15% moisture content range that is typical for small grain hay products).

Estimating soil moisture trends in cropped and fallow fields

Soil samples (339 samples in total) were collected prior to planting, at harvest, and at various time points throughout the season for a total of nine sampling dates in the 2023–24 season and seven dates in the 2024–25 season. We collected soil at 12-inch depth increments to 36 inches (0–12 in., 12–24 in., 24–36 in.). Samples represented 47 environment-date combinations, with one of the environments being a fallow field adjacent to the experimental plots. We then calculated soil water content as a percentage of soil volume (or volumetric water content) by recording the change in sample weight after oven drying and factoring in soil physical properties (i.e., bulk density). We calculated total soil water content as the sum of water content values across depths.

Forage water productivity for different planting dates

Water productivity is a way of expressing the amount of output from a crop (e.g., biomass or cash returns) per unit of a given input—in this case, applied water. We calculated forage water productivity as pounds per acre of soft dough forage harvested per unit of total water applied to the crop, with total water including precipitation and irrigation. We then used statistical models to test the impact of 1) irrigation treatment (irrigated or rainfed), 2) planting date, and 3) season (dry or average) on the water productivity of the forage.

Seasonal changes in soil water content

Using our estimates of soil water content for the various environment-date combinations, we averaged across samples and estimated changes in soil water content from March to June. Separate estimates were made according to whether the field was irrigated, rainfed, or fallow, and statistical models were used to determine the impact of field type on the soil water content at a given time during the season.

Supplementary Results

In the accompanying report, we present results for establishment irrigated forage water productivity for the 2023–24 and the 2024–25 growing seasons at the WSREC site. Figure B2 presents these results again with the inclusion of the rainfed crop treatment. While years with sufficient rainfall—such as the 2023–24 season—can generate reasonable forage yields even without irrigation input, in years with low rainfall (e.g., the 2024–25 season) both crop and water productivity were low. In 2024–25, the rainfed crop did not germinate until late November and it was harvested for forage just before it was starting to fail. In contrast, even in the low rainfall conditions, the establishment irrigated treatments produced efficient forage outcomes in the 2024–25 season. These results highlight how relying on rainfall alone does not necessarily result in the most efficient water use outcomes. Even small amounts of supplemental irrigation can greatly improve yield outcomes, allowing for higher productivity from limited water inputs and reduced risk of crop failure.

We measured additional experimental components that are not included in this technical appendix or the accompanying report. These will be presented in forthcoming work. Some key takeaways: 1) In comparison to forage outcomes, grain outcomes were more variable, with lower productivity and higher risk of crop failure; 2) Crop type and variety choice are important considerations. The best crop type for forage versus grain products or for early-planted, establishment irrigated crops versus purely rainfed crops are not the same. While some generalities about the crop species can be made, variety selection for the specific growing conditions and harvest product is a more important factor.

FIGURE B2

Water productivity for two growing seasons and irrigation treatments at WSREC

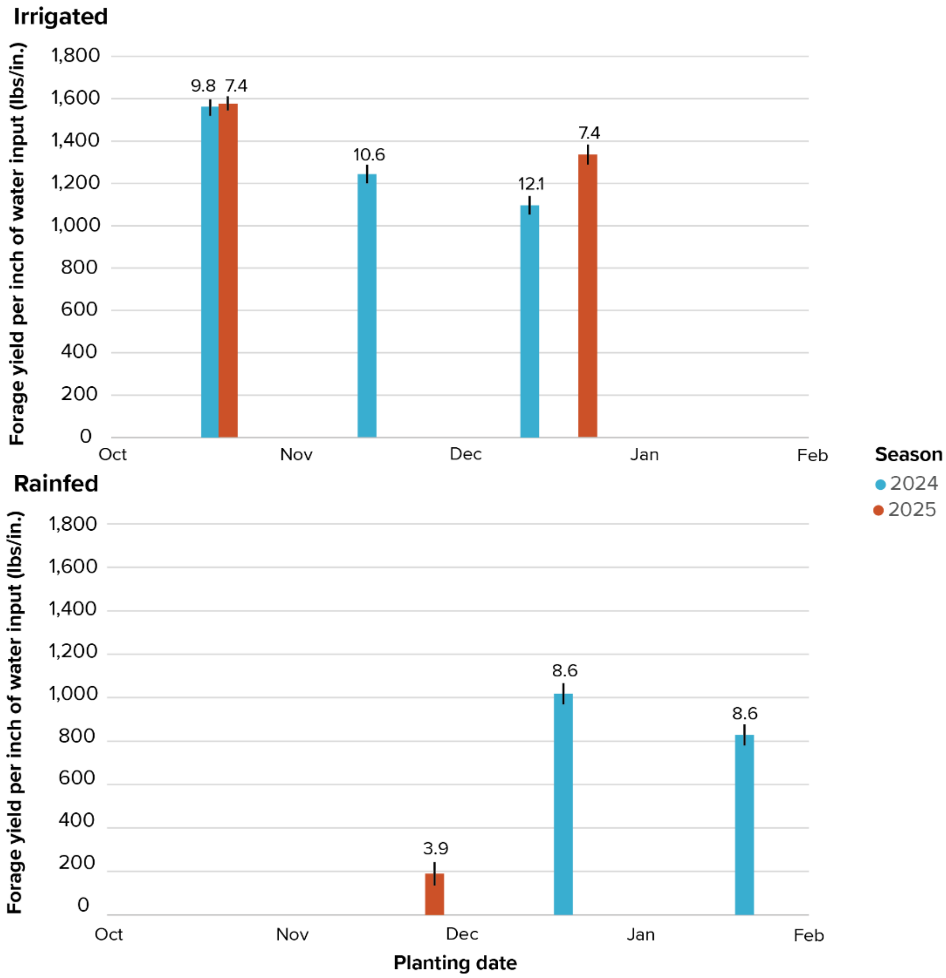

SOURCE: Author measurements.

NOTES: Yields were measured for a University of California winter grain variety trial in western Fresno County in two winter growing seasons: 2023–24 (a near-average rainfall year at this site) and 2024–25 (a dry year). Labels above bars indicate total water input (rainfall + irrigation; in.) from planting through forage harvest. Forage water productivity is calculated as pounds of winter wheat forage yield per inch of water input on a per-acre basis. Error bars show ±1 standard error.

Figure B3 compares soil moisture dynamics between fallow fields and cropped fields for the establishment irrigated and rainfed treatments in both seasons. While the rainfed field shows a soil water deficit relative to the fallow fields beginning in April in both years, the establishment irrigated field does not show a deficit until May. In the near-normal rainfall season of 2023–24, both the rainfed and irrigated crops had depleted soil moisture relative to the fallow by about 1.5 inches. In the dry 2024–25 season, soil water contents equalized among the three treatments by June and were not significantly different. This result highlights the importance of earlier forage harvests (e.g., in March/early April) for preserving soil moisture under water-limited conditions. It also illustrates that small, temporary soil water surpluses or deficits among treatments tend to resolve as fallow fields lose more water later in the season.

FIGURE B3

Late-season soil water content for two growing seasons and three field types at WSREC

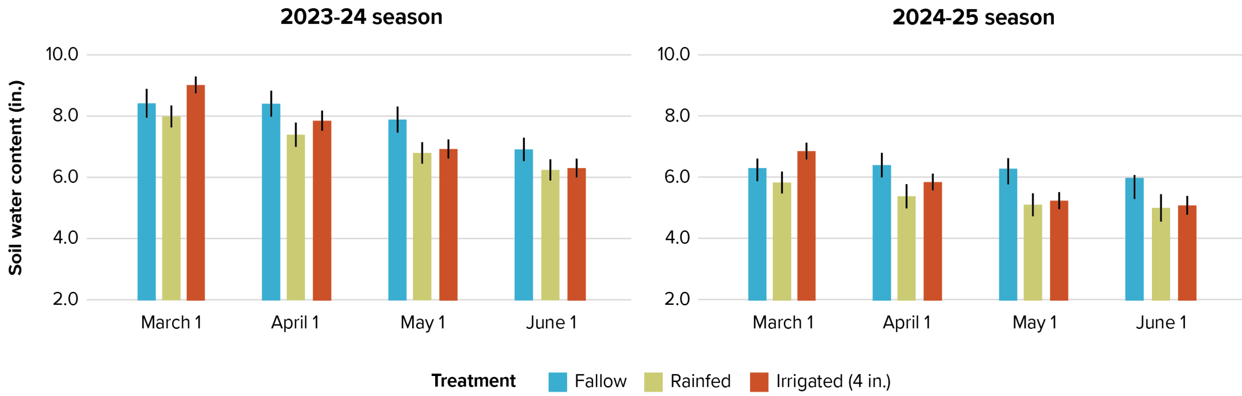

SOURCE: Author measurements.

NOTES: Late-season (March through June) soil water content (in.) to 3-foot depth in a fallow field, a winter cropped field established with 4 inches of irrigation ("irrigated 4 in."), and a non-irrigated ("rainfed") winter cropped field for a University of California small grain variety trial in western Fresno County. Results are averaged across three planting dates (early, mid, and late). Winter 2023–24 was a near-average rainfall year, while winter 2024–25 was a dry year.

Appendix C. Modeled Water Balances for Fallowed Fields and Low-Water Winter Forages

Introduction

Under California's Sustainable Groundwater Management Act (SGMA), pumping restrictions will likely result in anywhere from 500,000 to 900,000 of farmland in the San Joaquin Valley being removed from irrigated production. Transitioning to cropping systems that keep farmland in production with much less water can help soften the economic and social impacts of farmland fallowing, ideally offering multiple benefits—such as income generation, soil protection, or improved recharge—while meeting the sustainability goals of local groundwater agencies.

Previous PPIC and University of California research has described one such option: minimally irrigated winter crops that can produce forage for California's large livestock industry (Peterson, Pittelkow, and Lundy 2022 and 2023). Key to the uptake of these systems in the current regulatory landscape is understanding the effect of water-limited winter crops on field-level water balances relative to leaving the land fallow. Local rules and regulations often assume that bare fallow ground is the most efficient way to capture rainfall for storage in the soil or underground aquifers. But this assumption neglects the many interactions between plants and the soil—such as surface shading, infiltration, and rooting channels—that could impact the water balance in cropped versus fallowed fields.

Water applied to a field, whether rainfall or irrigation, can have one of several fates: it can evaporate directly to the atmosphere from the soil surface, be taken up by the plant and then released to the atmosphere via transpiration, stay in the soil profile, or drain to groundwater aquifers.[1] The analyses described in Technical Appendices A and B to the report *SGMA-Ready Crops as a Low-Water Alternative to Fallowing* provide some insight into evaporation and transpiration of applied water in cropped vs. fallow fields via direct and remotely sensed measurements. But the belowground elements of the water balance—infiltration into soil storage or deep drainage to groundwater—are more difficult to measure directly.

In this appendix, we describe our approach for using crop and soil hydraulic models to better illuminate possible outcomes for the belowground elements of the water balance. The two key questions we address are:

- Do fallow fields contribute positively to groundwater levels by capturing rainfall that then drains to aquifers? Would winter crops be detrimental to water balances by using rainfall for transpiration and crop growth instead?
- Similarly, are winter crops detrimental to rainfall capture and storage in the soil profile?

The results of this exercise, along with the best management practices described in the report and Technical Appendix B, are helpful for understanding the scenarios when water-limited forages are most appropriate as a land use alternative to fallowing.

Cropping system and soil water models for estimating forage growth and water balances

To understand the impact of water-limited winter forage crops on each component of the soil water balance we used two public domain model environments: the Agricultural Production Systems sIMulator (APSIM Next Generation; Holzworth et al. 2018) and HYDRUS 1D (version 4.17.0140, Šimůnek et al., 2020). APSIM is a

[1] We assume that runoff and lateral movement of applied water are negligible.

widely validated agricultural modeling framework that uses biophysical and human management elements to represent complex farming systems. But it relies on a cascading water balance approach that simplifies water distribution across different soil layers. HYDRUS 1D, developed by the U.S. Salinity Laboratory, is a physically based vadose zone model that employs the Richard's equation and van Genuchten model to solve for variably saturated flow in one dimension (van Genuchten 1980). However, HYDRUS 1D is more limited in its ability to simulate crop related processes.

Pairing these two models allowed us to combine APSIM's strength in crop physiological processes (e.g., crop growth and yield) with HYDRUS 1D's greater ability to predict water flow through the soil. This approach enabled representation of soil water processes based on physical properties while avoiding the complexity and numerical instability associated with fully coupled plant-soil models.

We used the following workflow to develop model inputs and scenarios for analysis:

1. Calibrate APSIM using observed data on soil moisture and forage yields;
2. Calibrate HYDRUS and optimize soil parameters using observed soil hydraulic properties and soil moisture data;
3. Generate APSIM outputs for a 25-year continuous simulation of forage production and potential ET under historical weather conditions and selected management systems;
4. Use these outputs to inform HYDRUS calculations of actual ET based on soil moisture conditions over the same 25-year simulation period and develop field-level water balance summaries.

Field sites and soil model configuration

Data on soil water content, hydraulic properties, and forage growth and yield were collected from two experimental field sites: the UC ANR West Side Research and Extension Center (WSREC) near Five Points, CA, and the Center for Irrigation Technology (CIT) at Fresno State University in Fresno, CA. Water-limited crop variety trials were conducted at these sites over two years for two cropping treatments (fallow or cropped with winter cereals), two irrigation treatments (four inches of establishment irrigation or rainfed) and three planting dates (early, mid, and late). At both sites we collected data on soil moisture content and hydraulic properties at various time points throughout the growing season. Full details on experimental design and crop trial methods for the WSREC site are provided in Technical Appendix B. The CIT trial replicated a subset of these treatments for the same two years. We also used forage yield measurements from the 2017–18 season at WSREC as an independent test set.

The two sites represent contrasting soil types with distinct soil hydraulic parameters: a clay loam and a sandy loam at WSREC and CIT, respectively. We assumed that vertical soil profiles extended to 6.5 feet (2 meters) deep for each site, with crop root density linearly declining with depth from the surface to 3.3 feet (1 meter) depth.

At WSREC, the modeled profile contained three aggregated layers (0–16 in., 16–40 in., and 40–80 in.) and at the CIT site, the profile contained two aggregated layers (0–50 in. and 50–80 in.). Layers were aggregated based on similar soil textures from measured field data down to 3.3 feet, and at WSREC using additional data from Neilson et al. (1964). For WSREC, we used these aggregated layers to implement an inverse modeling routine within HYDRUS 1D to optimize selected hydraulic parameters. Because soil moisture content data for CIT was limited, we were unable to calibrate this site for soil moisture. However, we did parameterize the model for CIT soil hydraulic properties based on soil water retention curves generated from samples at three depths across two replicated areas. Soil moisture over time was then modeled for 12 in., 24 in., 36 in., and 80 in. depths over time (Figure C1).

FIGURE C1

Cross section of soil profile showing depths for modeled soil moisture estimates

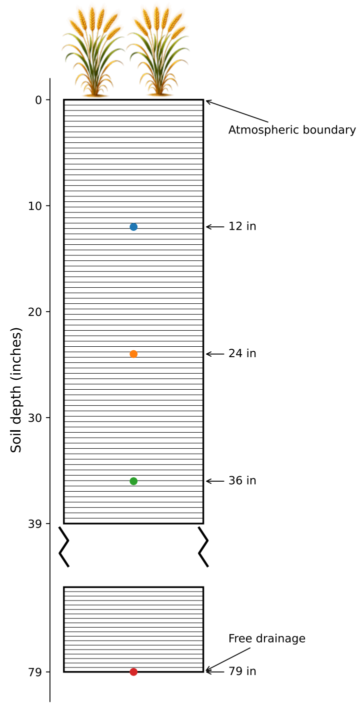

SOURCE: Author rendering.

NOTES: Colored dots represent the depths for which soil moisture was estimated using HYDRUS-1D paired with APSIM crop yield and ET outputs. "Atmospheric boundary" refers to the boundary between the soil and the air, where vapor exchange occurs. Free drainage refers to the depth below which we assume water returns to groundwater aquifers as recharge and is appropriate for very deep water tables.

APSIM crop growth calibration

We used APSIM to simulate winter wheat production and evapotranspiration (ET) for the soil, weather conditions, and crop management protocols at WSREC and CIT. Soil physical properties were determined using NRCS Web Soil Survey values where field measurements were not available (Soil Survey Staff n.d.). Model weather inputs included historical precipitation and minimum and maximum temperature for 2000–2025 from CIMIS and PRISM, and incoming solar radiation from the LaRC POWER database (Stackhouse 2010). Simulated fields were configured to closely replicate actual management practices and treatment structures at the field trials, including planting date and irrigation treatments, sowing depth and density, and fertilizer applications.

We compared observed data with model predictions for soil water and winter wheat forage yield from the 2023–24 and 2024–25 seasons at CIT and WSREC, as well as the 2017–18 season at WSREC. APSIM includes an extensive library of wheat cultivars with considerable differences in agronomic productivity under California growing conditions; however, there is not yet a validated APSIM wheat variety for a California-specific winter wheat variety. We iterated over a wide range of spring-type winter wheat varieties available in the APSIM library—either off-the-shelf or with targeted modifications—to determine the variety that produced yield predictions closest to observed yields in the field.

The best-aligned variety produced yield estimates with a relative root mean squared error (rRMSE) of 24 percent, meaning the model was able to capture over three-quarters of the variability in observed measurements (Figure C2 and C3). The model tended to underpredict yields for establishment irrigated treatments and overpredict yields for rainfed treatments. This should be considered when interpreting our results for water balances discussed in the next section: the model likely overestimates water use by crops in the rainfed scenario, and underestimates water use by crops in the establishment irrigated scenario. Because we did not have observed data to compare with model estimates for the fully irrigated treatment, this scenario should be considered an illustration that offers a basis of comparison for water-limited cropping systems against conventional, fully irrigated systems.

FIGURE C2

APSIM predicted biomass compared to observed field trial data (time series)

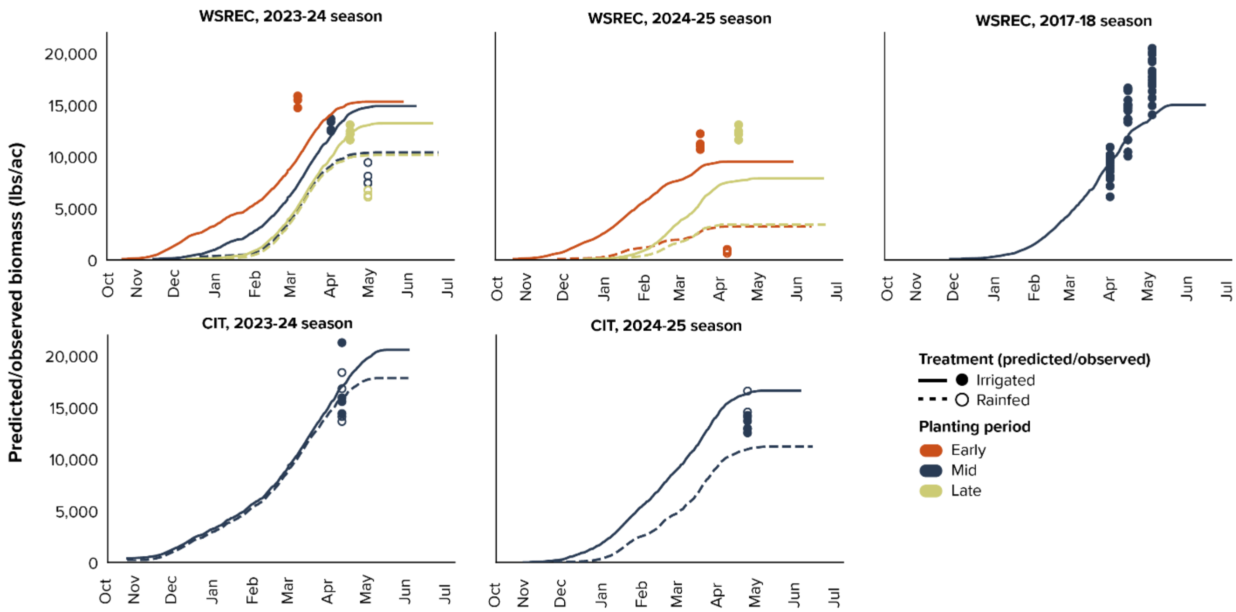

SOURCES: University of California field trials at WSREC and CIT in Fresno County (observed biomass yields); APSIM outputs (simulated biomass yields).

NOTES: Points represent observed winter wheat biomass from three seasons at WSREC and two seasons at CIT in Fresno County. Multiple points on a given sampling date are for measurement replicates. Lines represent predicted wheat biomass outputs from the APSIM model (lbs. per acre).

FIGURE C3
APSIM performance for yield predictions of establishment irrigated and rainfed wheat forage

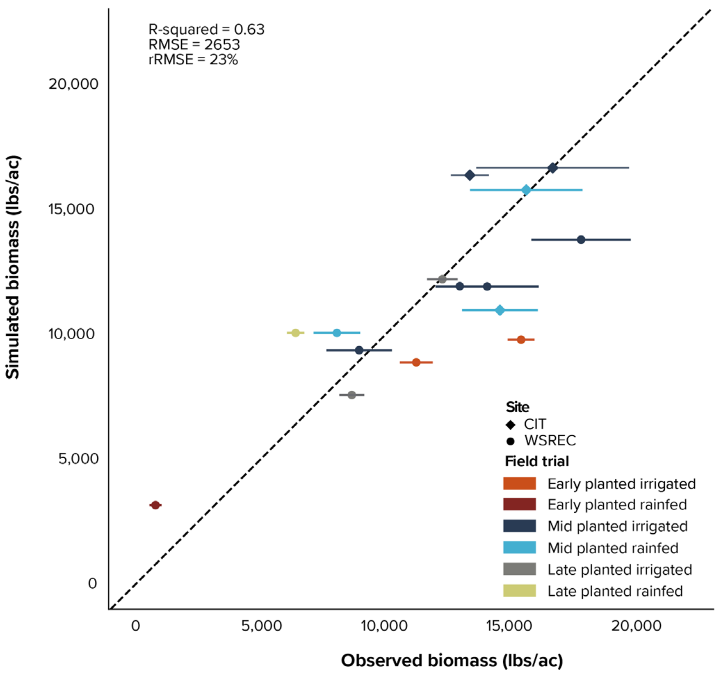

SOURCES: University of California field trials at WSREC and CIT in Fresno County (observed biomass yields); APSIM outputs (simulated biomass yields).

NOTES: Simulated treatments included establishment irrigated (3.5 inches) and rainfed wheat with early, mid, and late planting dates. The diagonal line represents perfect 1:1 alignment between observed and simulated yields. Values to the right of the line indicate model underpredictions of yield, while values to the left of the line indicate model overpredictions. Horizontal lines represent ±1 standard deviation. R-squared is the coefficient of variation; root mean squared error (RMSE) is the average difference between simulated and observed yields (lbs. per acre); relative RMSE (rRMSE) is a unitless expression of RMSE that indicates the proportion of variation that is not explained by the model.

HYDRUS 1D soil physical properties calibration

HYDRUS 1D requires soil hydraulic parameters to solve the Richards Equation. These parameters include residual soil water content (Θ_r), saturated water content (Θ_s), saturated hydraulic conductivity (K_s), the air entry parameter, alpha (α), and the shape fitting parameter (n). Values for these parameters were determined using measured soil water retention curve data collected with HYPROP and WP4C instruments (Meter Group) for 0–6 in. and 6–12 in. depths at WSREC and 0–12 in., 12–18 in., and 18–36 in. depths at CIT. The estimated soil hydraulic parameters for the fallow plot at WSREC were further calibrated against observed soil moisture data at 0–12 in., 12–24 in., and 24–36 in. depths using the built-in inverse modeling routine within HYDRUS 1D. Calibration was conducted on the fallow field to isolate soil hydraulic behavior from the impacts of plant growth; we later validated these estimates with a subset of observed data from a planted field.

Modeled soil moisture outputs were extracted from observation nodes that matched the field observation depths for direct comparison. Selected soil hydraulic parameters—including K_s and n—were estimated for each depth increment using the Marquardt-Levenberg optimization algorithm to minimize differences between modeled and measured soil moisture contents (Simunek and van Genuchten 1999). Observed soil moisture data were weighted equally across depths and time points.

Calibration was conducted over a representative period spanning October 2023 to March 2025, and the resulting optimized parameters were used for subsequent simulations. The RMSE for water content of the three layers in the fallow field at WSREC was 0.05, 0.02, and 0.01 for 0–12 in., 12–24 in., and 24–36 in. depths, respectively, with an overall R^2 of 0.57 (Figure C4).

FIGURE C4

HYDRUS 1D performance for predicting soil water content in fallow fields

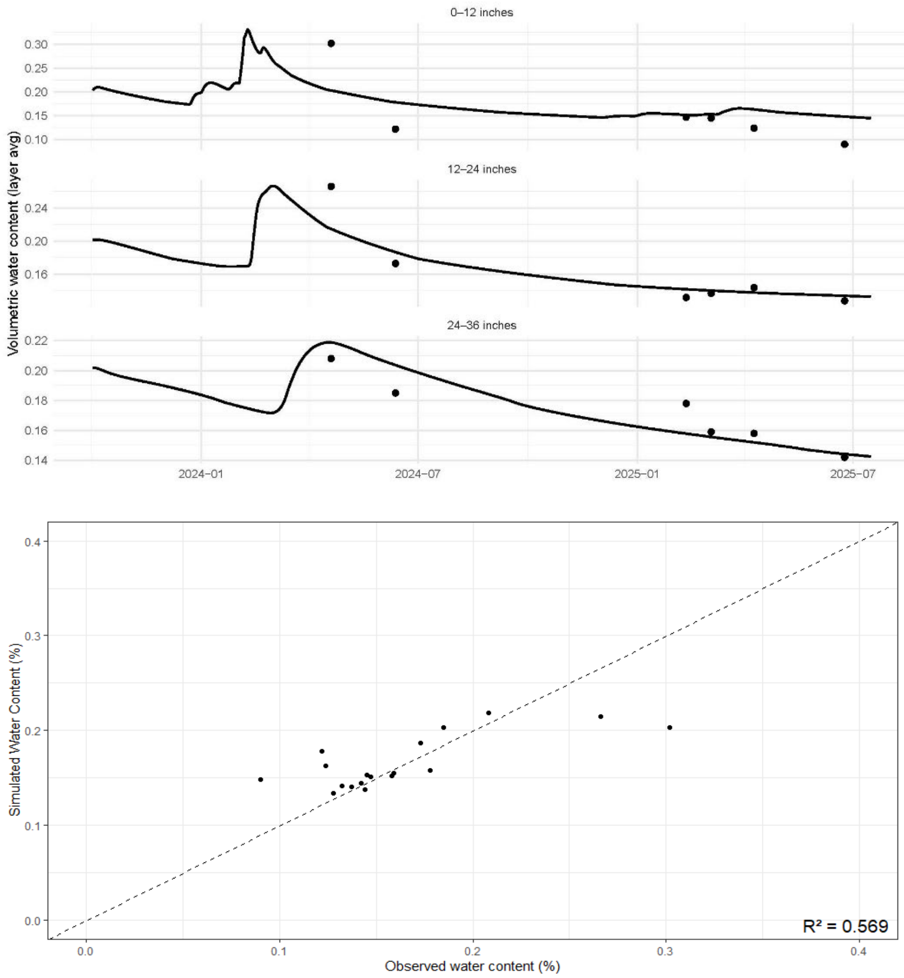

SOURCES: University of California field trials at WSREC in Fresno County (observed soil moisture); HYDRUS 1D outputs (simulated soil moisture).

NOTES: The top panel shows predicted and observed soil moisture content in a fallow field. Soil moisture was recorded intermittently at three depths from 2023–25. Solid lines are HYDRUS-predicted moisture contents; points represent observed soil moisture at these depths. The bottom panel shows the relationship between simulated and observed soil water content, with the diagonal line representing perfect 1:1 alignment between observed and simulated yields. R-squared is the coefficient of variation.

The calibrated model was then validated for a cropped field using a subset of observed soil water observations to understand how the calibrated soil hydraulic parameters performed when a crop was present spanning the same time period. The RMSE for soil moisture was 0.07, 0.07, and 0.09 for 0–12 in., 12–24 in., and 24–36 in. depths, respectively. The model tended to perform better for shallow layers compared to deeper layers. The overall R^2 was 0.50.

FIGURE C5

HYDRUS 1D performance for predicting soil water content in cropped, establishment irrigated fields

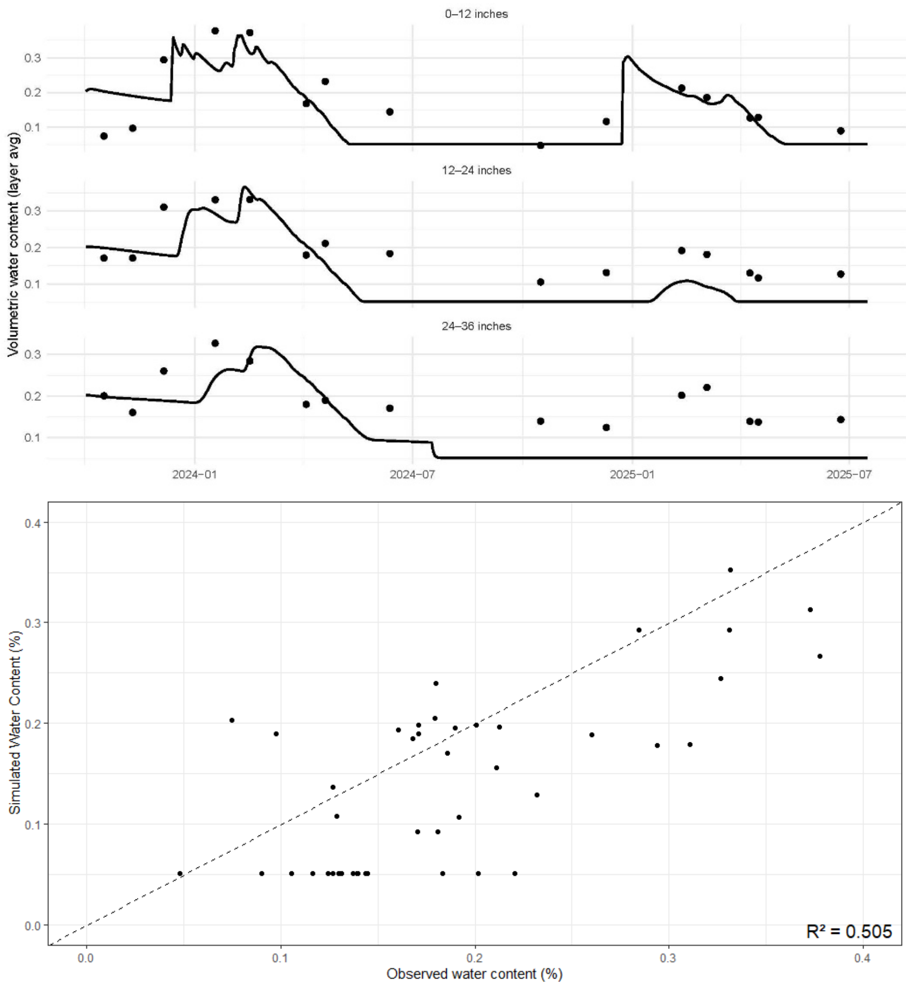

SOURCES University of California field trials at WSREC in Fresno County (observed soil moisture); HYDRUS 1D outputs (simulated soil moisture).

NOTES: The top panel shows predicted and observed soil moisture content in cropped fields that received 3.5 inches of establishment irrigation. Soil moisture was recorded intermittently at three depths from 2023–25. Solid lines are HYDRUS predicted moisture contents; points represent observed soil moisture at these depths. The bottom panel shows the relationship between simulated and observed soil water content, with the diagonal line representing perfect 1:1 alignment between observed and simulated yields. R-squared is the coefficient of variation.

Linking long-term simulations of wheat forage growth, ET, and soil water balance

Once calibrated, we used APSIM to simulate daily crop growth, potential soil evaporation (E_o), and potential plant transpiration (E_{op}) from cropped and fallow fields for 25 years of historical weather at the two sites. We ran the 25-year simulations for the following scenarios:

- Fallow field (evaporation only)
- Rainfed wheat harvested for forage
- Establishment irrigated (4 inches) wheat harvested for forage
- Fully irrigated wheat harvested for grain.

For each cropped scenario we also ran simulations for early (October 15), middle (November 15), and late (December 15) planting dates. We implemented crop germination and establishment rules based on average plant-available soil water over a 5-day moving window. Crop germination required an average soil water content of 30 percent, and establishment required average soil water content of 15 percent for 25 days after germination. If soil moisture was too low to allow crop germination or establishment, we considered this a failed crop. The establishment irrigated treatment was given 4 inches of water immediately after sowing, while the fully irrigated treatment received 4-inch applications upon reaching growth-stage-specific soil moisture thresholds, up to a maximum of 20 inches of total applied water. All cropped treatments were fertilized as needed to avoid nitrogen limitation.

The resulting crop growth and ET predictions were used as bounding inputs for HYDRUS 1D. Actual soil evaporation, root water uptake, and deep percolation fluxes were calculated in HYDRUS 1D as a function of soil hydraulic properties and daily soil water status. Runoff was not simulated, but ponding at the surface layer was allowed. Root water uptake was simulated using the Feddes reduction function (Feddes et al. 1978), allowing transpiration to be reduced below potential rates under water-limited conditions. Similarly, potential soil evaporation was limited by surface soil moisture conditions to force the model to arrive at actual soil evaporation. Weather data from the nearest CIMIS stations were used for precipitation input data.

We then replicated the above simulation scenarios for the same 2000–25 period of historical weather, with the first five years treated as an initialization period and discarded. For each year, each component of the soil water balance was summarized: water inputs as precipitation and irrigation, water lost as evaporation, water lost as transpiration (water uptake), water drained below two meters (percolation/recharge), and changes in soil storage over time.

Field-level water balance and summer drydown

To understand the difference in soil water balances across treatments, we summarized HYDRUS 1D outputs within water year types. Years were binned by water year type—either, dry, normal, or wet—based on the 25th, 50th, and 75th percentiles of precipitation across the 20-year simulation period. Total water input (rainfall + irrigation), transpiration, evaporation, and recharge were then averaged within water years for fallow and cropped treatments. We presented the results of this exercise for normal rainfall years in the accompanying report; below we also present results for wet and dry years and for rainfed and fully irrigated treatments (Figure C6).

The results show how the impacts of water-limited crops on soil water balance can vary depending on the water year type. In dry years, minimally irrigated and rainfed crops will likely deplete soil water relative to fallow. In contrast, in wet years the minimally irrigated forage retained slightly more water in soil storage than the fallow: 4.6 inches vs. 3.3 inches. In normal and wet years, the proportion of water input that was retained as recharge was nearly equal or marginally more in the minimally irrigated forage crop compared to fallow. Overall, the forage crop used slightly more water than the fallow in most years but was not detrimental—and in some cases marginally improved—recharge and soil water storage.

FIGURE C6

Soil water balance for cropped and fallow fields across water year types

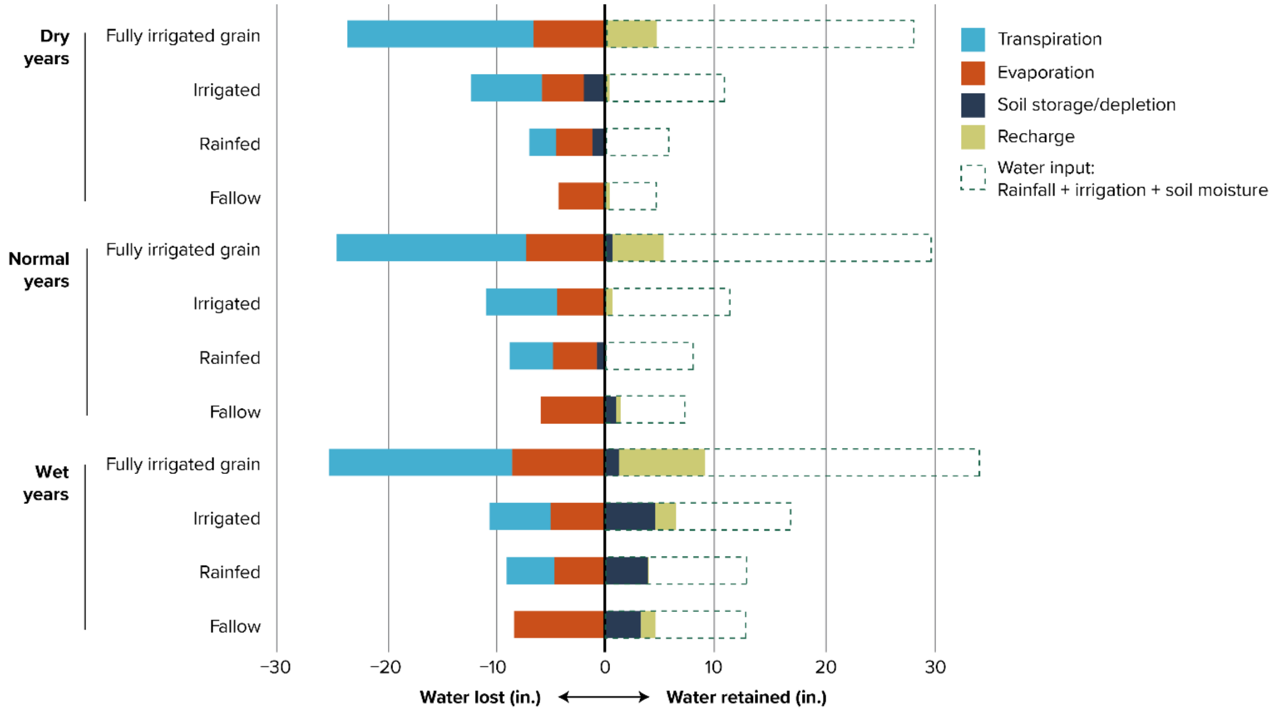

SOURCE: Author-simulated field-level water balances from HYDRUS 1D outputs.

NOTES: Rainfall amounts were derived from historical weather conditions from 2000–25. Water year types were binned by percentile of total annual precipitation. Dashed boxes represent total water input, including rainfall, irrigation, and sometimes extracted soil water (in.) summed across the growing season. The growing season extended from October through March for the irrigated and rainfed treatments, and through June 1 for the fully irrigated grain treatment. The stacked bars represent water that is either lost or gained from this total input amount. Losses can include transpiration (crop water uptake), evaporation (water lost from the soil surface), and soil water extracted by the crop; gains can include recharge (deep drainage to groundwater) and soil water storage, or water added to the soil profile by rainfall or irrigation. Values are the weighted average of years in a given water year type (dry, normal, or wet) across three planting dates (early, mid, and late).

Next we assessed cumulative water losses (evaporation and transpiration combined) and cumulative percolation (recharge) by treatment over the entire length of the simulation period (Figure C7). This exercise makes it easier to discern differences among the cropped and fallow treatments by tracking how their impact accrues over many years.

By the end of the 20-year simulation (the first 5 years were discarded as an initialization period), all but the fully irrigated scenario had very little cumulative percolation, ranging from nearly 0 to just over 30 inches. Cumulative water lost to evaporation and transpiration was lowest in the fallow scenario: roughly 14 feet. However, water losses in the rainfed and establishment irrigated scenarios were only about 8 inches more for the same period. Water loss in the fully irrigated grain scenario was roughly 20 inches more than the establishment irrigated forage scenario.

A few key takeaways emerge: first, direct groundwater recharge from rainfall represents only a small contribution to overall groundwater levels, and minimally irrigated crops make little difference—whether positive or negative—to this total. And second, total water losses from fallow fields—even when summed across two decades—are nearly the same as losses from minimally irrigated forage cropped fields. Additional losses from the cropped fields amounted to only a few inches over the course of 20 years.

FIGURE C7

Cumulative water gains (percolation) and losses (ET) after twenty years of fallow or minimally irrigated forages

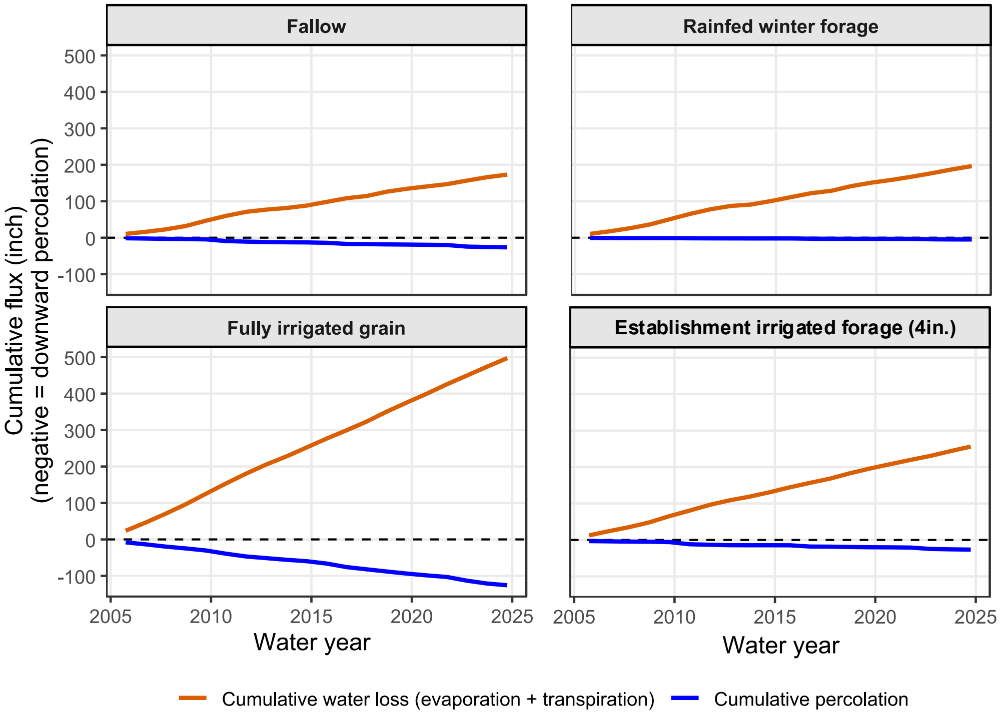

SOURCE: Author-simulated field-level water balances from HYDRUS 1D outputs.

NOTES: Cumulative water losses (evaporation and transpiration) and gains (percolation, or groundwater recharge) after 20 years of simulated management scenarios: fully irrigated and harvested for grain; minimally irrigated (four inches) at establishment and harvested for forage; rainfed and harvested for forage; and fallow. Negative fluxes represent downward percolation to groundwater, i.e., a gain for the overall water balance of the field. Cumulative water balance was calculated for full water years, from October 1 to September 31.

Most of the results in the accompanying report discuss soil water outcomes by the end of the forage harvest window, just as crop water consumption is at its peak. By focusing on this window, we hoped to show how targeted management practices—principally the timing of planting and harvest—can keep water use at a minimum while enabling a productive output from land that would otherwise be fallow. However, this begs a related question: what happens to water left in the soil after forage harvest? Does this water carry over into the fall planting season? Or is it lost to evaporation during California's hot, dry summer season? This question is particularly pertinent in the case of winter-planted fields left fallow in the summer due to lack of water for irrigation.

We used HYDRUS to simulate possible soil water outcomes by the end of the summer for the same management scenarios examined above. We found that, in most years, any soil water surpluses at the time of forage harvest had largely disappeared by the end of the summer whether the field was cropped or fallow. Figure C8 shows the percent difference in soil water content by the end of the summer, relative to water content at the beginning of the water year (October 1). For establishment irrigated forage crops, only the driest years end with less water in the soil than when they started, and then only by roughly 5 percent. Fallow fields may gain soil water during the rainy season, but typically return to about the same water content as they started with (or within 1–3 percent) by the end of summer.

FIGURE C8

Soil water content is highly variable during the winter rainy season, but tends to return to a low baseline by the end of summer

SOURCE: Simulated soil water content from HYDRUS 1D outputs.

NOTES: Shown is the percent difference in soil water content from the beginning to the end of each water year, averaged across water year types (dry, normal, or wet) for each management scenario. The dotted vertical line indicates the harvest date for the rainfed and establishment irrigated forage scenarios. The dotted rectangle indicates the harvest window for the fully irrigated grain scenario. Water year types were determined by percentile of cumulative precipitation from October 1 to March 31 (for forage and fallow scenarios) or to mid-June (for the grain scenario).

It is likely that summer-season management practices—such as mulching or leaving standing residue in the field after forage harvest—could reduce water loss to evaporation during the summer. However, our results indicate that most gains in soil water storage are temporary when viewed on an annual basis.

An important caveat to these results is the degree of precision that is possible for modeled estimates of soil water dynamics, which are difficult to measure and validate in the field. Our results represent outputs from models calibrated for two sites with contrasting soil types on the east and west sides of Fresno County. Given that results for cropped and fallow fields often differ by no more than a few percentage points, these results should be treated as illustrative and a first step towards better understanding in-field water balances for SGMA-ready management alternatives.

REFERENCES

Abatzoglou, John T. 2011. "Development of Gridded Surface Meteorological Data for Ecological Applications and Modelling." *International Journal of Climatology* 33(1), 121–131.

Allen, Richard G., Luis S. Pereira, Dirk Raes, and Martin Smith. 1998. *Crop evapotranspiration: Guidelines for computing crop water requirements*. FAO Irrigation and Drainage Paper No. 56. Rome: Food and Agriculture Organization of the United Nations.

Bates, D., M. Mächler, B. Bolker, and S. Walker. 2015. "Fitting Linear Mixed-Effects Models Using lme4." *Journal of Statistical Software* 67(1): 1–48.

DWR. 2024. "Statewide Crop Mapping—California Natural Resources Agency Open Data" [dataset]. California Department of Water Resources.

DWR. 2026. "California Irrigation Management Information System (CIMIS)" [dataset]. California Department of Water Resources.

Escriva-Bou, Alvar, Ellen Hanak, Spencer Cole, and Josué Medellín-Azuara. 2023. *The Future of Agriculture in the San Joaquin Valley*. Public Policy Institute of California.

Feddes, R. A., P. J. Kowalik, and H. Zaradny. 1978. "Simulation of field water use and crop yield." In *Simulation Monographs*, eds. F. W. T. Penning de Vries and H. H. van Laar (Pudoc).

Holzworth, Dean, et al. 2018. "APSIM Next Generation: Overcoming Challenges in Modernising a Farming Systems Model." *Environmental Modelling & Software* 103:43–51.

Lenth, R. 2025. "emmeans: Estimated Marginal Means, aka Least-Squares Means" R package version 1.11.2-00002.

Melton, Forrest S., et al. 2021. "OpenET: Filling a Critical Data Gap in Water Management for the Western United States." *Journal of the American Water Resources Association* 58 (6): 971–994.

Nielsen, D. R., J. M. Davidson, J. W. Biggar, and R. J. Miller. 1964. "Water movement through Panoche Clay Loam soil." *Hilgardia* 35 (17): 491–506.

Peterson, Caitlin, Cameron Pittelkow, and Mark Lundy. 2022. *Exploring the Potential for Water-Limited Agriculture in the San Joaquin Valley*. Public Policy Institute of California.

---. 2023. "Targeted irrigation expands scope for winter cereal production in water-limited areas of California's San Joaquin Valley." *Agricultural Systems* 210:103696.

Pinheiro, J. C., and D. M. Bates. 2000. *Mixed-Effects Models in S and S-PLUS*. Springer.

PRISM Climate Group. n.d. "PRISM Time Series Data." [dataset]. Oregon State University. Accessed March 26, 2026.

R Core Team. 2025. *R: A language and environment for statistical computing. R Foundation for Statistical Computing*. R Foundation for Statistical Computing.

Šimůnek, J., and M. Th. van Genuchten. 1999. "Using the HYDRUS-1D and HYDRUS-2D Codes for Estimating Unsaturated Soil Hydraulic and Solute Transport Parameters. In *Characterization and Measurement of the Hydraulic Properties of Unsaturated Porous Media*. 2nd Edition, 1523–1536.

Šimůnek, J., M. Šejna, and M. Th. van Genuchten. 2020. "Hydrus 1D - archive of version 4.16.0110" [Software]. HydroShare.

SSURGO. 2026. "Web Soil Survey" [dataset]. Soil Survey Staff, Natural Resources Conservation Service, United States Department of Agriculture. Accessed January 15, 2026.

Stackhouse, P. W. 2010. "Prediction of Worldwide Energy Resources" [dataset]. National Aeronautics and Space Administration.

USGS. 2026. "Landsat Spectral Indices." [dataset]. US Geological Survey Earth Resources Observation and Science Center.

van Genuchten, M. Th. 1980. "A Closed-Form Equation for Predicting the Hydraulic Conductivity of Unsaturated Soils." *Soil Science Society of America Journal* 44 (5): 892–898.

Volk, John M., et al. 2024. "Assessing the Accuracy of OpenET Satellite-Based Evapotranspiration Data to Support Water Resource and Land Management Applications." *Nature Water* 2 (2): 193–205.

Wickham, H. 2016. *ggplot2: Elegant Graphics for Data Analysis*. Springer-Verlag.

PUBLIC POLICY INSTITUTE OF CALIFORNIA

The Public Policy Institute of California is dedicated to informing and improving public policy in California through independent, objective, nonpartisan research.

Public Policy Institute of California
475 Sansome Street, Suite 1150
San Francisco, CA 94111
T: 415.291.4400
F: 415.291.4401
PPIC.ORG/WATER

PPIC Sacramento Center
1215 K Street, Suite 1740
Sacramento, CA 95814
T: 916.440.1120
F: 916.440.1121